

A New Generic Progressive Approach based on Spectral Difference for Single-sensor Multispectral Imaging System

Vishwas Rathi¹^a, Medha Gupta²^b and Puneet Goyal¹^c

¹Department of Computer Science and Engineering, Indian Institute of Technology Ropar, Rupnagar, Punjab, India

²Department of Computer Science and Engineering, Graphic Era University, Dehradun, India

Keywords: Multispectral Imaging System, Image Demosaicking, Multispectral Filter Array, Color Difference, Interpolation, Spectral Correlation.

Abstract: Single-sensor RGB cameras use a color filter array to capture the initial image and demosaicking technique to reproduce a full-color image. A similar concept can be extended from the color filter array (CFA) to a multispectral filter array (MSFA). It allows us to capture a multispectral image using a single-sensor at a low cost using MSFA demosaicking. The binary tree based MSFAs can be designed for any k-band multispectral images and are preferred, however the existing demosaicking methods are either not generic or are of limited efficacy. In this paper, we propose a new generic demosaicking method applicable on any k-band MSFAs, designed using preferred binary-tree based approach. The proposed method involves applying the bilinear interpolation and estimating the spectral correlation differences appropriately and progressively. Experimental results on two different multispectral image datasets consistently show that our method outperforms the existing state-of-art methods, both visually and quantitatively, as per the different metrics.

1 INTRODUCTION

The energy transmitted from light origins or reflected by objects contains a wide range of wavelengths. The standard color image contains the scene's information in only three bands: Red, Green and Blue. However, a multispectral image has more than three spectral bands, which makes the multispectral image more informative about the scene than the standard color image. Therefore, multispectral images are found useful in many research areas such as remote sensing (MacLachlan et al., 2017), medical imaging (Zenteno et al., 2019), food industry (Qin et al., 2013; Chen and Lin, 2020), satellite imaging (Mangai et al., 2010) and computer vision (Ohsawa et al., 2004; Vayssade et al., 2020; Junior et al., 2019). Depending on the application, there are different requirements of information captured through multiple spectral bands. These multiple requirements in different domains motivated the manufacturer to develop different multispectral imaging (MSI) systems (Fukuda et al., 2005; Thomas et al., 2016; Geelen et al., 2014; Pichette

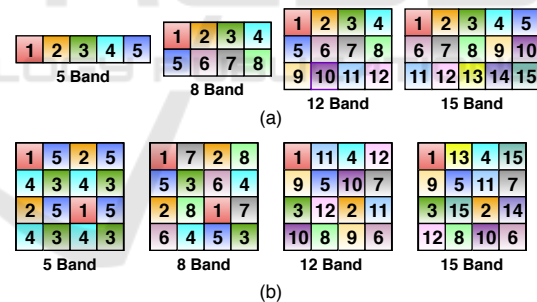


Figure 1: MSFA designs. (a) Non-redundant MSFAs used in (Brauers and Aach, 2006; Gupta and Ram, 2019). (b) Binary-tree based MSFAs defined in (Miao and Qi, 2006).

et al., 2016; Ohsawa et al., 2004; Monno et al., 2015) of varying bands.

The concept of the single-camera-one-shot system is recently getting explored to develop low-cost multispectral imaging systems using the MSFA similar to the standard color camera that also uses a single sensor to capture three bands' information with a CFA. The image captured using a single-camera-one-shot system records only one spectral band information at each pixel location and this image is called a mosaic image or MSFA image in the multispectral domain. A complete multispectral image is generated

^a <https://orcid.org/0000-0002-6770-6142>

^b <https://orcid.org/0000-0001-6013-3719>

^c <https://orcid.org/0000-0002-6196-9347>

from an MSFA image using an interpolation method called MSFA demosaicking. This single-sensor multispectral imaging system (SSMIS) would be of low cost and small size, and can also capture videos in the multispectral domain.

However, MSFA demosaicking is a challenging task because of the highly sparse sampling of each spectral band. As the number of spectral bands in a multispectral image increases, the spatial correlation is lower in the image. That is why SSMIS considering only spatial correlation does not perform well on higher spectral bands multispectral images. Further, the quality of the multispectral image generated using SSMIS depends on the demosaicking method and the MSFA pattern used to capture the mosaic image. As there is no such de-facto standard for MSFA design similar to the Bayer pattern in the RGB domain, the MSFA pattern choice becomes crucial. The binary tree based MSFAs that can be designed for any k -band multispectral images, are preferred (Miao and Qi, 2006; Gupta and Ram, 2019). Also, as the requirement of the number of spectral bands is application-specific, it motivates the need for development of a generic MSFA demosaicking method for wider applicability. This research, therefore, aims to develop a generic MSFA demosaicking method for SSMIS using binary tree based MSFAs to provide better quality multispectral images. The existing generic MSFA demosaicking methods (Miao et al., 2006; Brauers and Aach, 2006) fail to generate good quality multispectral images, especially for higher band multispectral images. The other MSFA demosaicking methods (Mihoubi et al., 2017; Monno et al., 2015; Monno et al., 2012; Monno et al., 2011; Jaiswal et al., 2017) are restricted to multispectral images of some specific band size.

This paper proposes an MSFA demosaicking method utilizing both the spatial and spectral correlation in the MSFA image. The proposed method is generic, i.e., not restricted for any specific number of spectral band images. It uses the binary-tree based MSFA patterns (Miao and Qi, 2006), which are considered most compact and designable for any number of bands. The proposed method first interpolates the missing pixel by performing progressive bilinear interpolation, explicitly designed for binary-tree based MSFA pattern. Then these interpolated bands are used progressively in the spectral correlation difference method. Experimental results on multiple benchmark datasets show that the proposed method outperforms other state-of-the-art generic MSFA demosaicking methods, both visually and quantitatively.

2 RELATED WORK

In this section, we discuss different MSFA patterns present in the literature and associated MSFA demosaicking methods.

2.1 Different MSFA Patterns

We divide the MSFA patterns into two categories, as shown in Figure 1, depending on the probability of appearance (PoA) of bands in the MSFA pattern.

1. There are many MSFA designs (Brauers and Aach, 2006; Mihoubi et al., 2015; Aggarwal and Majumdar, 2014) where each band has equal PoA in the MSFA pattern. Brauers and Aach (Brauers and Aach, 2006) proposed a six-band non-redundant MSFA pattern which stores bands in 3×2 matrix. This was later extended and the generalized designs for non-redundant MSFA patterns were presented (Gupta and Ram, 2019). Also, Aggarwal and Majumdar (Aggarwal and Majumdar, 2014) proposed uniform and random MSFA pattern design; both of these are generic and can be extended to capture any number of bands multispectral images. Mihoubi et al. (Mihoubi et al., 2015) used square non-redundant MSFA design for the 4, 9, and 16-band images.
2. Another category of MSFA design is binary-tree based where MSFA is more compact and the several spectral bands can have different PoA in the MSFA pattern. Miao and Qi (Miao and Qi, 2006) proposed this binary-tree based generic method to generate MSFA patterns using a binary tree for any number of bands multispectral images. These are more preferred compared to redundant ones and many of the recent works have used binary-tree based MSFAs (Miao and Qi, 2006). Monno et al. in his works (Monno et al., 2012; Monno et al., 2011; Monno et al., 2014; Monno et al., 2015) used five-band MSFA pattern where, PoA of G-band is kept 0.5.

2.2 MSFA Demosaicking

The method (Brauers and Aach, 2006) extended the color-difference-interpolation of CFA demosaicking to the multispectral domain. But it failed to generate quality multispectral images. Further, (Mizutani et al., 2014) improved Brauers and Aach method by iterating demosaicking methods multiple times. The number of iterations depended on the correlation between two spectral bands.

Miao et al. (Miao et al., 2006) proposed a binary tree-based edge sensing (BTES) generic method for

MSFA demosaicking that used the MSFA patterns generated using (Miao and Qi, 2006). BTES method used the same binary tree for interpolation, which is used to design MSFA pattern. BTES performed edge sensing interpolation to develop a complete multispectral image. Although BTES is generic, it does not perform well on a higher band multispectral image as it uses only spatial correlation.

In (Aggarwal and Majumdar, 2014), authors used uniform MSFA design for MSFA demosaicking and proposed a linear demosaicking method that requires the prior computation of parameters using original images. This limits the feasibility and applicability of the method as original images would not be available in real-time situation. Mihoubi et. al. (Mihoubi et al., 2015) used the concept of intensity image, which has a strong spatial correlation with each band than bands considered pairwise. Further, Mihoubi et al. in (Mihoubi et al., 2017) had improved their previous work by proposing a new estimation of intensity image. However, their method is not generic.

Monno et. al. (Monno et al., 2015; Monno et al., 2012; Monno et al., 2011; Monno et al., 2014) proposed several methods considering the MSFAs designed using the binary-tree based method and used the concept of guide image which was generated from under sampled G-band, and later they used this guide image as a reference to interpolate remaining under-sampled bands. (Monno et al., 2011) extended existing upsampling methods to adaptive kernel upsampling methods using an adaptive kernel to reconstruct each band and later improved in (Monno et al., 2012) using the guided filter. To further improve (Monno et al., 2012), in (Monno et al., 2015), the authors constructed multiple guide images and used them for interpolation. This approach is not effective for a higher band multispectral image. It is limited to the MSFA pattern where G-band has PoA 0.5, making other bands severely undersampled in higher band multispectral image. (Jaiswal et al., 2017) also utilized the MSFA generated using (Monno et al., 2015). Here, authors proposed a method using frequency domain analysis of spectral correlation for five-band multispectral images. This method requires the complete information of multispectral images for the model's learning parameters estimation, which would not be available in real practice for MSFA based multispectral camera device intended to be developed.

Few machine learning and deep learning-based MSFA demosaicking methods (Aggarwal and Majumdar, 2014; Shopovska et al., 2018; Habtegebrail et al., 2019) also has been recently explored. However, these methods require atleast some of the original multispectral images of the SSMIS for the learn-

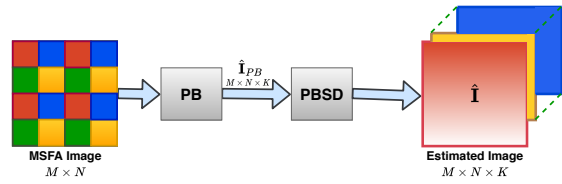


Figure 2: Proposed MSFA demosaicking approach.

ing and training of model parameters, but that will not be available in the real world capturing scenario for the considered SSMIS.

3 PROPOSED METHODOLOGY

In this paper, we propose an MSFA demosaicking method that is based on progressive bilinear interpolation and progressive bilinear spectral difference. As shown in Figure 2, the complete method essentially comprises of two steps, mentioned as follows:

1. First, interpolate the missing pixel values using a progressive bilinear (PB) approach designed specifically for the binary tree based MSFA patterns.
2. Second, use progressive bilinear spectral difference (PBSD) approach based on inter-band differences and applied progressively.

In the following subsections 3.1 and 3.2, we present these steps in more details.

3.1 Progressive Bilinear (PB) Interpolation

Here, we describe a new intra-band progressive approach for estimating the missing pixel values at a few unknown locations using the bilinear interpolation on some initially known pixel values, as per the binary-tree based MSFA and the specific spectral band considered. Then, these estimated pixel values with initially known pixel values are used to calculate missing pixel values at other locations. PB interpolation approach consists of the following components.

3.1.1 Pixel Selection

PB interpolation is an intra-band approach and thus independent of the order of bands selected for the interpolation. But the order of pixel locations chosen for the interpolation for the different bands is different. This pixel selection order critically depends on the binary tree used to create the MSFA pattern, designed using (Miao and Qi, 2006). For any chosen

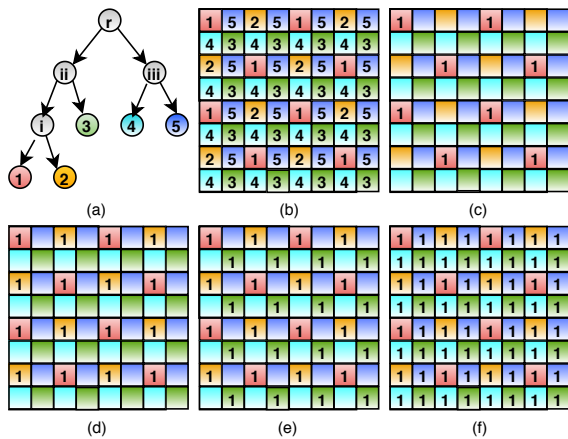


Figure 3: Illustration of PB interpolation of band 1. (a) Binary tree used to generate 5-band MSFA. (b) 5-band MSFA pattern for 8×8 size mosaic (raw) image. (c) Band 1's pixel locations in the original mosaic image; one may note that band 1's PoA = $1/8$ initially. (d) Band 1 estimated first at the locations of a band corresponding to sibling node, i.e., band 2, using filter F_4 . (PoA now = $1/4$) (e) Later, interpolate at the locations of band 3 using filter F_1 (Band 1 PoA now = $1/2$) (f) Finally, interpolate at the locations of band 4 and 5 using filter F_2 .

$$\frac{1}{4} \begin{bmatrix} 1 & 0 & 1 \\ 0 & 0 & 0 \\ 1 & 0 & 1 \end{bmatrix}; \frac{1}{4} \begin{bmatrix} 0 & 1 & 0 \\ 1 & 0 & 1 \\ 0 & 1 & 0 \end{bmatrix}; \frac{1}{4} \begin{bmatrix} 1 & 0 & 0 & 0 & 1 \\ 0 & 0 & 0 & 0 & 0 \\ 0 & 0 & 0 & 0 & 0 \\ 0 & 0 & 0 & 0 & 0 \\ 1 & 0 & 0 & 0 & 1 \end{bmatrix}; \frac{1}{4} \begin{bmatrix} 0 & 0 & 1 & 0 & 0 \\ 0 & 0 & 0 & 0 & 0 \\ 1 & 0 & 0 & 0 & 1 \\ 0 & 0 & 0 & 0 & 0 \\ 0 & 0 & 1 & 0 & 0 \end{bmatrix};$$

F_1 F_2 F_3 F_4

Figure 4: Filters used for PB interpolation.

band during interpolation, we first estimate the missing band information at the sibling band's pixel locations and move one level up in the binary tree and repeat the same process until we estimate the missing band information at all locations. If the sibling node is an internal node, then the bands corresponding to the leaves under the sibling node can be considered in any order. For example, consider the binary tree for a 5-band multispectral image and corresponding MSFA pattern-based mosaic image, as shown in Figure 3(a) and (b), respectively. For interpolating band 1, we can select the pixel locations either in the order: $\{2,3,4,5\}$ or $\{2,3,5,4\}$. For interpolating band 3, we can select the pixel locations either in the order: $\{1,2,4,5\}$, $\{2,1,4,5\}$, $\{1,2,5,4\}$ or $\{2,1,5,4\}$, and for interpolating band 4, we must first select pixel locations corresponding to band 5 and then locations for the other bands 1, 2 and 3 in any order.

3.1.2 Interpolation

Given the pixel selection order for a band, the missing pixel values of this band are progressively in-

terpolated using the four closest known neighboring pixel values of the same band. This closest neighborhood, at any progressive step, depends on the PoA of the known (original and/or estimated) pixel values of the selected band. For the binary-tree based MSFA patterns, it can be observed that the 3×3 neighborhood of a missing data pixel will contain at least four known pixels if PoA of the band considered is greater than or equal to $1/4$, and for the band pixels with PoA less than $1/4$ but greater than or equal to $1/16$, four known neighboring pixels will lie in 5×5 neighborhood. Based on the locations of the known neighboring pixels in the closest neighborhood, we select the filter and perform convolution at pixel locations of the selected band in the pixel selection scheme. The filters are shown in Figure 4, and can work up to 16 bands multispectral image. In Algo. 1, we define the interpolation scheme, which interpolates band q at other band locations. The same algorithm can be repeated to interpolate all the bands of the multispectral image. In Figure 3(c), to interpolate band 1 at some location (i,j) of band 2, four nearest pixel values of band 1 are found in 5×5 neighborhood at locations $(i-2,j)$, $(i+2,j)$, $(i,j-2)$, and $(i,j+2)$. Therefore, F_4 filter is used to interpolate band 1 at locations of band 2. After interpolating at band 2 locations, PoA of band 1 increases to $1/4$, as shown in Figure 3(d), which makes four nearest pixel values of band 1 to be available in 3×3 neighborhood. Further, to interpolate band 1 at locations of band 3, we use filter F_1 and finally, we use filter F_2 to interpolate at band 4 and 5 locations.

Algorithm 1: Interpolation scheme for band- q .

Input: I_{MSFA}, F, M_B, q

- 1 $\tilde{I}^q = I_{MSFA} \odot m^q$ // Initialization
- 2 For each band p taken in the order given by pixel selection scheme, repeat following steps 3 and 4;
- 3 Select F_i based on current PoA of \tilde{I}^q
- 4 $\tilde{I}^q = \tilde{I}^q + (\tilde{I}^q * F_i) \odot m^p$
- 5 $\hat{I}_{PB}^q = \tilde{I}^q$

where, I_{MSFA} is K band mosaic image of size $M \times N$, $F = \{F_1, F_2, F_3, F_4\}$ is set of filters used, $M_B = \{m^1, \dots, m^K\}$ is set of K binary masks, each of size $M \times N$, '*' is convolution operator, and ' \odot ' is element wise multiplication operator. The binary mask m^q has value 1 only at locations where q^{th} band's original values are there.

3.2 Progressive Bilinear Spectral Difference (PBSD)

The PBSD method is applicable for any binary-tree based MSFAs and thus it can be used to interpolate any K-band images using PB interpolation. It is motivated from color difference based interpolation method (Brauers and Aach, 2006). Using $\hat{\mathbf{I}}_{PB}$ as the initial multispectral image, the following steps are performed to generate the interpolated $\hat{\mathbf{I}}$ multispectral image.

1. For each ordered pair (p, q) of bands, determine the sparse band difference \tilde{D}^{pq} at q^{th} band's locations.

$$\tilde{I}^q = I_{MSFA} \odot m^q \quad (1)$$

$$\tilde{D}^{pq} = \hat{I}_{PB}^p \odot m^q - \tilde{I}^q \quad (2)$$

2. Now compute the fully-defined band difference \hat{D}^{pq} using PB interpolation of \tilde{D}^{pq} . Computing this on binary tree based MSFAs is feasible only because of the new approach i.e. PB, as described in subsection 3.1.
3. For each band q , estimate \hat{I}^q at pixel locations where $m^p(x, y) = 1$ as:

$$\hat{I}^q = \sum_{p=1}^K (\tilde{I}^p - \hat{D}^{pq} \odot m^p) \quad (3)$$

Now, all K bands are fully-defined and together form the complete multispectral image $\hat{\mathbf{I}}$.

4 EXPERIMENTAL RESULTS

We implement the proposed method PBSD and examine its performance on two publicly available multispectral image datasets: (a) Cave dataset (Yasuma et al., 2010) and (b) TokyoTech dataset (Monno et al., 2015). The Cave dataset contains 31 images each of having 31-bands, and these bands range from 400nm to 700nm with a spectral gap of 10nm. The TokyoTech dataset contains 30 images. Each image has 31-bands, and the spectral range of these 31-bands is from 420nm to 720nm with a spectral gap of 10nm. We consider multispectral images with band size (K) varying from 5 to 15. The K-band multispectral images were prepared from these 31-band images by selecting K-bands at equal spectral gaps beginning from the first band. We obtain the mosaic image by sampling the pixel values based on the MSFA pattern defined for each band and then applying the MSFA demosaicking method to estimate the complete multispectral image.

We compare the proposed method with other existing generic MSFA demosaicking methods: WB (Gupta and Ram, 2019), SD (Brauers and Aach, 2006), LMSD (Aggarwal and Majumdar, 2014), ISD (Mizutani et al., 2014), IID (Mihoubi et al., 2015), and BTES (Miao et al., 2006). We consider CIE D65 illumination for the evaluation of methods. To compare the estimated image's quality with the original image, we evaluate these methods based on the PSNR and SSIM image quality metrics.

Figure 5 represents the quantitative performance of different methods. For many larger bands images, the SD and ISD methods seem to perform better than the BTES method. However, the BTES method, using compact (binary-tree based) MSFAs, performs better for some bands such as 5, 7, 11, and 13. The sharp decrease in the performance for the 5, 7, 11, and 13 band images in WB, SD, and ISD methods is because of the non-compact characteristics of the non-redundant MSFAs used in these methods. This observation was the motivation for the proposed method. For seven and higher bands multispectral image, the proposed method PBSD performs consistently better than the other methods, including BTES and LMSD, on both datasets considered. This may be noted that the IID method is applicable only to the non-redundant MSFA pattern of square size (e.g. 2×2 , 3×3 , or 4×4). Thus its results are shown here in Figure 5 for only 9-band multispectral images.

Tables 1 and 2 represent reconstruction results for 8, 11 and 14 band multispectral images using different MSFA demosaicking methods. It can be observed that the proposed method PBSD performing better and provides 1-2 dB average PSNR improvement in compared to second best performing method. Table 3 shows the overall average PSNR and SSIM values taken over different bands (5-band to 15-band) multispectral images. The existing method BTES performs reasonably better than other existing methods, however the proposed method PBSD performs the best by providing further improvement of 1.25 dB in PSNR and around 0.9% in SSIM on BTES on the Cave dataset and 1.21 dB in PSNR and 2.5% in SSIM on the TokyoTech dataset images.

Figure 6 shows the visual comparison of the few images from the Cave and TokyoTech datasets generated by the various MSFA demosaicking methods for 7 and 14 band multispectral images. To estimate colorimetric accuracy, we convert the K-band multispectral images into the sRGB domain using (Monno et al., 2015). We select smaller portions from multiple images so that artifacts should be visible. We can observe that other existing MSFA demosaicking methods generate significant artifacts on the text of the im-

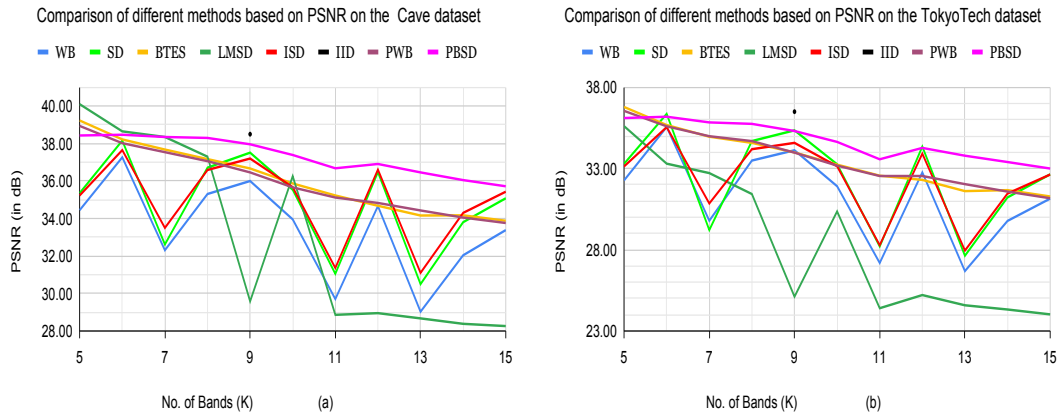


Figure 5: Comparison of different MSFA demosaicking methods based on PSNR (a and b) on the Cave and TokyoTech datasets. There are a few other MSFA demosaicking methods (Monno et al., 2015; Mihoubi et al., 2017; Jaiswal et al., 2017) as well, but these are not generic and therefore not considered for comparison.

Table 1: Comparison of PSNR(dB) values for different methods on 31 multispectral images of the Cave dataset.

Image	8-band						11-band						14-band					
	WB	BSD	BTES	LMSD	ISD	PBSD	WB	BSD	BTES	LMSD	ISD	PBSD	WB	BSD	BTES	LMSD	ISD	PBSD
Balloon	40.56	42.10	42.45	42.38	41.58	43.56	33.95	35.61	40.25	32.08	35.74	41.61	36.84	38.90	39.20	31.48	38.84	40.73
Beads	27.28	28.00	28.39	27.15	26.67	28.99	21.49	21.84	27.05	21.30	21.51	27.76	23.99	24.91	26.19	20.47	24.00	27.16
Cd	37.58	37.78	39.34	34.12	36.52	38.43	32.33	32.53	37.81	29.20	31.76	36.50	34.88	35.38	37.37	26.59	34.02	36.72
Chart&toy	29.92	31.60	31.60	34.32	32.01	33.50	25.17	26.96	29.67	24.54	27.59	32.08	27.20	29.35	28.54	24.05	30.45	30.89
Clay	36.81	37.31	41.35	37.19	36.27	40.41	31.17	31.51	39.53	30.91	31.52	38.65	33.21	33.77	37.20	30.33	33.62	37.29
Cloth	29.14	30.73	29.84	30.27	31.39	31.99	25.19	26.32	28.77	24.80	27.15	30.92	26.83	28.71	28.11	24.60	30.15	30.85
Egy_statue	38.55	40.22	39.69	41.82	40.26	41.62	32.79	34.24	38.06	32.51	34.86	40.11	35.30	37.49	37.21	32.51	38.53	39.46
Face	38.88	40.38	40.62	41.63	40.21	41.55	33.09	34.65	38.60	31.84	34.89	40.05	35.72	37.86	37.42	31.37	38.35	39.37
Beers	39.42	40.18	40.55	39.98	39.73	40.69	33.04	34.08	38.27	29.85	34.30	38.87	35.68	37.14	36.95	29.23	37.51	38.35
Food	38.25	39.12	38.87	38.01	38.42	39.50	31.86	32.82	37.12	29.16	32.46	38.15	34.86	36.50	36.04	28.95	36.15	37.75
Lemn_slice	34.59	36.00	35.56	36.59	36.31	37.01	29.72	31.32	34.39	28.24	31.79	35.96	31.85	33.70	33.62	28.00	34.54	35.60
Lemons	38.17	39.92	40.31	42.25	40.50	42.04	33.43	35.44	37.98	31.41	35.94	40.19	35.26	37.50	36.70	30.83	38.44	39.11
Peppers	36.53	38.63	39.96	39.86	38.39	40.80	29.00	31.01	36.87	31.23	31.46	38.77	31.50	34.09	35.49	30.45	35.13	38.31
Strawberry	36.69	38.50	38.16	39.83	39.00	40.27	32.59	34.18	36.23	30.06	34.62	38.68	34.24	36.15	35.34	29.68	37.31	37.95
Sushi	37.12	38.50	37.81	38.05	38.71	39.35	32.51	33.99	36.18	29.43	34.57	38.39	34.20	36.02	35.11	28.99	36.98	37.74
Tomatoes	34.99	36.83	35.59	37.86	37.41	37.74	31.68	33.06	34.42	29.29	33.64	37.01	32.74	34.72	33.48	29.24	35.86	36.21
Feathers	30.73	32.46	33.39	33.23	32.38	35.01	24.63	26.09	31.46	26.99	26.60	33.60	27.08	28.93	30.47	26.46	29.68	32.94
Flowers	36.32	37.14	37.88	36.14	36.16	38.57	29.25	30.33	36.66	29.13	30.42	37.08	32.70	34.13	35.92	28.93	34.12	37.07
Glass_tiles	26.78	28.15	29.48	30.29	28.57	30.59	22.34	23.35	27.53	24.76	24.25	29.01	24.04	25.45	26.51	24.59	26.47	28.11
Hairs	38.65	40.66	40.41	42.94	41.26	42.65	33.41	35.52	38.41	32.89	36.39	41.00	35.92	38.40	37.48	32.52	39.51	40.32
Jelly_beans	28.48	30.53	30.22	31.19	30.78	32.67	22.28	24.37	28.78	23.17	24.83	31.49	25.12	27.41	28.00	22.93	28.29	30.94
Oil_paint	31.49	32.93	32.68	34.04	33.69	34.06	28.18	29.20	31.74	28.81	30.15	33.25	29.73	31.22	30.98	28.13	32.32	32.61
Paints	29.40	31.23	32.49	32.55	31.60	32.98	23.61	25.24	29.44	22.54	25.87	31.48	25.21	27.02	27.98	21.94	28.31	30.47
Photo&face	37.25	39.26	39.12	39.76	39.03	40.09	30.97	32.98	36.59	30.23	33.40	38.77	33.53	36.03	35.44	30.26	36.77	37.73
Pompoms	38.42	38.74	39.54	36.94	37.24	39.69	30.67	30.79	38.13	29.52	29.73	37.22	34.60	35.26	37.30	28.59	33.71	37.41
R&f Apples	40.92	42.49	43.26	44.31	42.86	44.54	35.36	38.10	40.63	32.59	38.66	42.70	37.43	39.88	39.33	32.23	40.58	41.75
R&f pepper	38.44	40.24	40.77	42.74	40.72	42.51	33.36	35.33	38.27	31.36	35.71	40.12	35.42	37.70	36.94	30.63	38.49	39.32
Sponges	35.96	36.66	38.98	37.14	35.74	38.46	29.45	29.73	36.56	28.09	29.78	35.74	32.10	32.91	34.69	27.19	32.43	35.04
Stuf_toys	37.87	38.92	39.51	37.05	37.53	39.68	29.32	30.34	36.81	27.23	30.41	37.39	32.99	34.80	35.85	26.69	34.61	37.41
Superballs	38.19	39.66	39.46	37.58	39.09	40.94	32.08	33.22	37.58	30.38	33.12	39.15	34.73	36.34	37.04	30.92	36.20	39.00
Thr_spools	31.17	33.21	34.93	39.06	34.29	37.40	26.83	28.38	32.37	31.07	29.12	35.30	28.27	30.21	31.28	31.12	31.78	34.08
Average	35.31	36.71	37.17	37.30	36.59	38.30	29.70	31.05	35.23	28.86	31.36	36.68	32.04	33.80	34.17	28.38	34.30	36.05

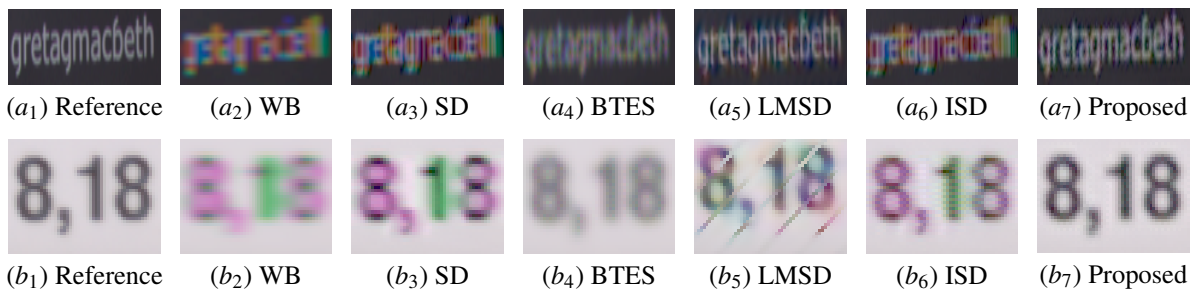


Figure 6: Visual comparison of demosaicked images (sRGB) generated from the 7-band (row a) and 14-band (row b) images.

Table 2: Comparison of PSNR(dB) values for different methods on 30 multispectral images of the TokyoTech dataset.

Image	8-band						11-band						14-band					
	WB	BSD	BTES	LMSD	ISD	PBSD	WB	BSD	BTES	LMSD	ISD	PBSD	WB	BSD	BTES	LMSD	ISD	PBSD
Butterfly	34.93	36.21	35.15	35.36	34.83	36.53	28.19	29.22	33.12	24.21	29.02	34.32	31.17	32.62	31.95	24.83	32.29	34.02
Butterfly2	29.54	29.34	30.1	28.19	29.06	29.95	23.1	23.18	27.83	21.82	23.3	28.13	25.42	26.02	27.17	21.38	26.37	27.83
Butterfly3	36.78	38.78	38.05	36.93	38.89	39.7	28.41	30.45	35.03	27.65	30.75	37.54	31.84	34.17	34.06	27.47	34.85	36.53
Butterfly4	36.49	38.71	37.21	38.15	38.54	39.72	29.85	31.39	34.66	27.26	31.57	37.75	32.47	34.54	33.69	28.36	35.01	37.02
Butterfly5	36.04	38.45	36.76	33.67	39.06	39.46	30.08	31.79	34.17	25.34	32.28	37.52	32.45	34.49	33.22	25.01	35.53	36.53
Butterfly6	32.66	34.14	33.88	33.13	34.53	35.55	25.94	27.21	31.37	24.04	27.55	33.88	28.53	30.17	30.54	24.11	31.15	33.05
Butterfly7	37.6	39.87	37.95	38.66	40.34	40.7	30.79	32.37	35.33	26.98	32.98	38.64	33.54	35.86	34.31	28.09	37.01	37.92
Butterfly8	35.5	38.3	36.01	36.92	38.05	39.32	28.7	30.59	34.04	26.28	30.72	37.64	31.71	34.2	33.08	26.57	34.66	36.61
CD	39.11	37.95	40.86	22.81	34.44	37.63	31.4	30.62	38.36	21.13	28.51	33.18	34.75	34.21	37.22	18.83	30.78	34.28
Character	29.25	33.54	30.88	33.37	34.94	35.13	22.08	23.97	27.61	20.28	24.64	32.65	24.26	26.66	26.35	20.23	27.97	31.15
Cloth	29.97	32.21	30.47	29.68	31.95	33.31	22.44	24.13	28.32	22.28	24.65	31.78	25.46	28.04	27.3	22.22	29.01	30.89
Cloth2	31.7	33.02	32.62	31.77	33.51	34.15	26.75	27.86	31.48	27.15	28.39	33.1	29.07	30.53	31.22	27.47	31.56	33.1
Cloth3	32.85	34.52	34.86	33.3	35.12	37.83	27.16	29.39	32.89	28.18	30.02	35.41	29.82	32.33	32.43	27.61	33.66	34.95
Cloth4	31.41	33.85	32.7	30.68	34.69	36.9	25.72	27.69	30.82	25.28	28.65	34.8	27.84	30.2	30.08	24.78	32.02	34.13
Cloth5	31.93	32.34	34.51	31.16	32.57	35.59	28.71	29.42	33.58	28.11	30.12	31.83	30.39	31.11	32.68	27.82	32.28	33.27
Cloth6	39.09	38.94	39.24	30.95	36.94	39.11	32.17	31.96	38.15	27.63	31.69	36.88	35.81	36.12	37.33	27.47	35.29	37.53
Color	42.37	40.62	40.38	36.5	39.04	37.66	47.01	44.17	36.36	24.54	41.79	34.42	42.1	40.76	34.94	24.51	39.15	34.4
Colorchart	41.91	41.74	44.73	33.31	38.89	42.19	31.57	32.25	41.87	27.72	31.25	39.16	36.1	37.22	40.24	27.66	35.4	39.31
Doil	25.12	26.28	25.86	27.03	26.37	27.42	20.82	21.6	24.85	21.11	22.08	26.05	22.69	23.92	24.29	21.1	24.57	25.99
Fan	26.38	27.38	27.06	27.06	26.99	28.33	20.58	21.63	25.71	20.06	22.06	27	23.15	24.45	24.84	20.12	24.88	26.36
Fan2	28.16	29.66	29.83	29.07	28.77	30.79	20.18	21.95	27.9	21.18	22.45	29.06	23.43	25.49	26.73	21.29	25.99	28.6
Fan3	27.79	29.3	29.35	29.36	28.8	30.57	20.54	22.01	27.44	21.72	22.43	28.96	23.47	25.42	26.54	21.46	26.08	28.52
Flower	41.78	42.07	43.55	27.82	39.56	43.31	32.41	32.64	41.77	24.49	31.67	40.79	37.29	38.36	41.21	24.4	36.92	41.69
Flower2	42.42	42.08	43.71	29.81	39.76	42.97	33.76	33.74	42.49	26.37	32.95	39.97	38.23	38.55	41.94	26.3	37.09	41.26
Flower3	43.16	42.76	44.17	30.02	40.13	43.13	33.05	33.63	42.42	26.63	32.93	40.5	37.89	38.91	41.72	26.58	37.49	41.37
Party	29.13	29.89	32.27	30.49	28.86	31.34	21.06	22.66	29.48	24.21	22.86	29.16	24.11	25.77	28.49	23.92	25.87	29.09
Tape	29.64	30.14	30.88	29.53	30.37	31.44	25.69	26.06	29.56	23.69	26.12	29.36	27.51	28.19	28.83	23.28	28.34	29.8
Tape2	32.13	33.38	32.48	33.93	33.35	33.64	27.06	28.92	31.07	25.91	29.35	30.89	28.84	29.83	30.11	25.74	30.38	31.37
Tshirts	24.14	27.06	24.65	25.92	27.87	28.63	18.75	20.45	23.14	18.45	21.39	27.37	20.81	23.42	22.4	18.71	25.27	26.73
Tshirts2	25.79	28.21	27.19	28.26	29.41	30.52	21.62	23.14	25.95	22.18	24.11	29.25	23.12	25.14	25.19	22.33	27.06	28.65
Average	33.49	34.69	34.58	31.43	34.19	35.75	27.19	28.20	32.56	24.40	28.28	33.57	29.78	31.22	31.67	24.32	31.46	33.40

Table 3: Comparison of different methods on the average over all bands (5-band to 15-band) images.

Cave	PSNR	WB	SD	BTES	LMSD	ISD	PWB	PBSD
		33.5	34.8	36.1	33.0	35.0	36.0	37.3
Tokyo-Tech	SSIM	0.95	0.96	0.97	0.92	0.96	0.97	0.98
	PSNR	31.3	32.4	33.5	28.3	32.3	33.5	34.7
	SSIM	0.91	0.92	0.94	0.83	0.93	0.95	0.96

ages, whereas our proposed method reproduces the sRGB images more accurately than the other methods.

5 CONCLUSIONS

The non-redundant MSFAs are not compact, and that limits the efficacy of MSFA demosaicking methods using such MSFAs. The binary tree based MSFAs are compact and facilitate better spectral and spatial correlation. However, most of the existing demosaicking methods using binary tree based (preferred) MSFAs are not generic. In this work, a novel progressive approach of demosaicking is presented that can be used for effectively reconstructing any K-band multispectral images from binary-tree based (compact) MSFAs. The proposed method is generic, and it applies initially bilinear interpolation appropriately and progressively and then uses the spectral differences method to further improve the quality of demosaicked image. We evaluated the proposed method's performance by comparing it with other existing generic MSFA demosaicking methods on multiple multispectral image datasets. Considering different performance metrics

and the visual assessment, the proposed method's performance is consistently observed better than the existing generic MSFA demosaicking methods. In the future, we plan to enhance and develop application-specific efficient MSFA demosaicking methods.

ACKNOWLEDGEMENTS

This research is supported by the DST Science and Engineering Research Board, India under grant ECR/2017/003478.

REFERENCES

Aggarwal, H. K. and Majumdar, A. (2014). Single-sensor multi-spectral image demosaicing algorithm using learned interpolation weights. In *Proceedings of the International Geoscience and Remote Sensing Symposium*, pages 2011–2014.

Brauers, J. and Aach, T. (2006). A color filter array based multispectral camera. In *12. Workshop Farbbildverarbeitung*, pages 55–64.

Chen, I. and Lin, H. (2020). Detection, counting and maturity assessment of cherry tomatoes using multi-spectral images and machine learning techniques. In *Proceedings of International Joint Conference on Computer Vision, Imaging and Computer Graphics Theory and Applications (VISIGRAPP)*, pages 759–766.

- Fukuda, H., Uchiyama, T., Haneishi, H. and Yamaguchi, M., and Ohya, N. (2005). Development of 16-band multispectral image archiving system. In *Proceedings of SPIE*, pages 136–145.
- Geelen, B., Tack, N., and Lambrechts, A. (2014). A compact snapshot multispectral imager with a monolithically integrated per-pixel filter mosaic. In *Proceedings of SPIE*, volume 8974, page 89740L.
- Gupta, M. and Ram, M. (2019). Weighted bilinear interpolation based generic multispectral image demosaicking method. *Journal of Graphic Era University*, 7(2):108–118.
- Habtegebrail, T. A., Reis, G., and Stricker, D. (2019). Deep convolutional networks for snapshot hyperspectral demosaicking. In *10th Workshop on Hyperspectral Imaging and Signal Processing: Evolution in Remote Sensing*, pages 1–5.
- Jaiswal, S. P., Fang, L., Jakhetiya, V., Pang, J., Mueller, K., and Au, O. C. (2017). Adaptive multispectral demosaicking based on frequency-domain analysis of spectral correlation. *IEEE Transactions on Image Processing*, 26(2):953–968.
- Junior, J. D., Backes, A. R., and Escarpinati, M. C. (2019). Detection of control points for uav-multispectral sensed data registration through the combining of feature descriptors. In *Proceedings of International Joint Conference on Computer Vision, Imaging and Computer Graphics Theory and Applications (VISIGRAPP)*, pages 444–451.
- MacLachlan, A., Roberts, G., Biggs, E., and Boruff, B. (2017). Subpixel land-cover classification for improved urban area estimates using landsat. *International Journal of Remote Sensing*, 38(20):5763–5792.
- Mangai, U., Samanta, S., Das, S. and Chowdhury, P., Varghese, K., and Kalra, M. (2010). A hierarchical multi-classifier framework for landform segmentation using multi-spectral satellite images-a case study over the indian subcontinent. In *IEEE Fourth Pacific-Rim Symposium on Image and Video Technology*, pages 306–313.
- Miao, L. and Qi, H. (2006). The design and evaluation of a generic method for generating mosaicked multispectral filter arrays. *IEEE Transactions on Image Processing*, 15(9):2780–2791.
- Miao, L., Ramanath, R., and Snyder, W. E. (2006). Binary tree-based generic demosaicking algorithm for multispectral filter arrays. *IEEE Transactions on Image Processing*, 15(11):3550–3558.
- Mihoubi, S., Losson, O., Mathon, B., and Macaire, L. (2015). Multispectral demosaicking using intensity-based spectral correlation. In *Proceedings of the 5th International Conference on Image Processing Theory, Tools and Applications*, pages 461–466.
- Mihoubi, S., Losson, O., Mathon, B., and Macaire, L. (2017). Multispectral demosaicking using pseudo-panchromatic image. *IEEE Transactions on Computational Imaging*, 3(4):982–995.
- Mizutani, J., Ogawa, S., Shinoda, K., Hasegawa, M., and Kato, S. (2014). Multispectral demosaicking algorithm based on inter-channel correlation. In *Proceedings of the IEEE Visual Communications and Image Processing Conference*, pages 474–477.
- Monno, Y., Kiku, D., Kikuchi, S., Tanaka, M., and Okutomi, M. (2014). Multispectral demosaicking with novel guide image generation and residual interpolation. In *Proceedings of IEEE International Conference on Image Processing*, pages 645–649.
- Monno, Y., Kikuchi, S., Tanaka, M., and Okutomi, M. (2015). A practical one-shot multispectral imaging system using a single image sensor. *IEEE Transactions on Image Processing*, 24(10):3048–3059.
- Monno, Y., Tanaka, M., and Okutomi, M. (2011). Multispectral demosaicking using adaptive kernel upsampling. In *Proceedings of IEEE International Conference on Image Processing*, pages 3157–3160.
- Monno, Y., Tanaka, M., and Okutomi, M. (2012). Multispectral demosaicking using guided filter. In *Proceedings of the SPIE Electronic Imaging Annual Symposium*, pages 829900–1–829900–7.
- Ohsawa, K., Ajito, T., Komiya, Y. and Fukuda, H., Haneishi, H., Yamaguchi, M., and Ohya, N. (2004). Six band hdtv camera system for spectrum-based color reproduction. *Journal of Imaging Science and Technology*, 48(2):85–92.
- Pichette, J., Laurence, A., Angulo, L., Lesage, F., Bouthillier, A., Nguyen, D., and Leblond, F. (2016). Intraoperative video-rate hemodynamic response assessment in human cortex using snapshot hyperspectral optical imaging. *Neurophotonics*, 3(4):045003.
- Qin, J., Chao, K., Kim, M. S., Lu, R., and Burks, T. F. (2013). Hyperspectral and multi spectral imaging for evaluating food safety and quality. *Journal of Food Engineering*, 118(2):157–171.
- Shopovska, I., Jovanov, L., and Philips, W. (2018). RGB-NIR demosaicing using deep residual U-Net. In *26th Telecommunications Forum*, pages 1–4.
- Thomas, J.-B., Lapray, P.-J., Gouton, P., and Clerc, C. (2016). Spectral characterization of a prototype sfa camera for joint visible and nir acquisition. *Sensor*, 16:993.
- Vayssade, J., Jones, G., Paoli, J., and Gee, C. (2020). Two-step multi-spectral registration via key-point detector and gradient similarity: Application to agronomic scenes for proxy-sensing. In *Proceedings of International Joint Conference on Computer Vision, Imaging and Computer Graphics Theory and Applications (VISIGRAPP)*, pages 103–110.
- Yasuma, F., Mitsunaga, T., Iso, D., and Nayar, S. (2010). Generalized assorted pixel camera: Postcapture control of resolution, dynamic range, and spectrum. *IEEE Transactions on Image Processing*, 19(9):2241–2253.
- Zenteno, O., Treuillet, S., and Lucas, Y. (2019). 3d cylinder pose estimation by maximization of binary masks similarity: A simulation study for multispectral endoscopy image registration. In *Proceedings of International Joint Conference on Computer Vision, Imaging and Computer Graphics Theory and Applications (VISIGRAPP)*, pages 857–864.